Brain, Behavior, and Immunity 121 (2024) 269–277

Contents lists available at ScienceDirect

Brain Behavior and Immunity

journal homepage: www.elsevier.com/locate/ybrbi

Full-length Article

Machine learning-driven diagnosis of multiple sclerosis from whole blood transcriptomics

Maryam Omrani [a,1], Rosaria Rita Chiarelli [a,1], Massimo Acquaviva [a,1], Claudia Bassani [a], Gloria Dalla Costa [a,b,c], Federico Montini [a,b,c], Paolo Preziosa [a,b,c], Lucia Pagani [d], Francesca Grassivaro [e], Simone Guerrieri [a,b], Marzia Romeo [a,b], Francesca Sangalli [a,b], Bruno Colombo [a,b], Lucia Moiola [a,b], Mauro Zaffaroni [f], Anna Pietroboni [g], Alessandra Protti [h], Marco Puthenparampil [e], Roberto Bergamaschi [i], Giancarlo Comi [a,b,c], Maria A. Rocca [a,b,c], Vittorio Martinelli [a,b], Massimo Filippi [a,b,c], Cinthia Farina [a,*]

[a] Institute of Experimental Neurology and Division of Neuroscience, IRCCS San Raffaele Scientific Institute, Milan, Italy
[b] Unit of Neurology, IRCCS San Raffaele Scientific Institute, Milan, Italy
[c] Vita-Salute San Raffaele University, Milan, Italy
[d] IQVIA, Analytics Center of Excellence, Milano
[e] Dipartimento di Neuroscienze, Azienda Ospedale – Università di Padova, Padova, Italy
[f] Centro Sclerosi Multipla, ASST della Valle Olona, Ospedale di Gallarate, Gallarate, Italy
[g] Fondazione IRCCS Cà Granda Ospedale Maggiore Policlinico, Milan, Italy
[h] ASST Grande Ospedale Metropolitano Niguarda, Milan, Italy
[i] IRCCS Fondazione Mondino, Pavia, Italy

ARTICLE INFO

Keywords:
Biomarkers
Clinically isolated syndrome
Machine learning
Multiple sclerosis
RNAseq
Whole blood

ABSTRACT

Multiple sclerosis (MS) is a neurological disorder characterized by immune dysregulation. It begins with a first clinical manifestation, a clinically isolated syndrome (CIS), which evolves to definite MS in case of further clinical and/or neuroradiological episodes. Here we evaluated the diagnostic value of transcriptional alterations in MS and CIS blood by machine learning (ML).

Deep sequencing of more than 200 blood RNA samples comprising CIS, MS and healthy subjects, generated transcriptomes that were analyzed by the binary classification workflow to distinguish MS from healthy subjects and the Time-To-Event pipeline to predict CIS conversion to MS along time. To identify optimal classifiers, we performed algorithm benchmarking by nested cross-validation with the train set in both pipelines and then tested models generated with the train set on an independent dataset for final validation.

The binary classification model identified a blood transcriptional signature classifying definite MS from healthy subjects with 97% accuracy, indicating that MS is associated with a clear predictive transcriptional signature in blood cells. When analyzing CIS data with ML survival models, prediction power of CIS conversion to MS was about 72% when using paraclinical data and 74.3% when using blood transcriptomes, indicating that blood-based classifiers obtained at the first clinical event can efficiently predict risk of developing MS.

Coupling blood transcriptomics with ML approaches enables retrieval of predictive signatures of CIS conversion and MS state, thus introducing early non-invasive approaches to MS diagnosis.

1. Introduction

Multiple sclerosis (MS) is a chronic inflammatory demyelinating disease of the central nervous system (CNS), characterized by profound heterogeneity in clinical course and progression (Marrie et al., 2022). The disease begins with a first clinical manifestation suggestive of MS, referred to clinically isolated syndrome (CIS) which evolves to definite MS in case of further clinical and/or neuroradiological episodes (Marrie

* Corresponding author.
E-mail address: farina.cinthia@hsr.it (C. Farina).
[1] M.O., R.R.C. and M.A contributed equally to this work.

https://doi.org/10.1016/j.bbi.2024.07.039
Received 9 April 2024; Received in revised form 23 July 2024; Accepted 28 July 2024

et al., 2022). The probability to diagnose MS changes depending on the applied diagnostic criteria, and has increased e.g. from McDonald criteria 2010 to Mc Donald criteria 2017, with 2017 criteria however suffering from low specificity as developed to maximise therapeutic care (Filippi et al., 2022). Thus, assessment of CIS conversion to MS may require time and imply costs for treatments, which represent a major economic burden in MS care (Bebo et al., 2022). While early diagnosis and treatment of the disease are important to prevent irreversible damage (Stankiewicz & Weiner, 2020), unnecessary exposure to drugs and adverse drug reactions in CIS subjects who will never progress to definite MS has to be avoided (Ng et al., 2024;Chung et al., 2020). For all these reasons, the identification of predictive factors measured at the first clinical event, possibly based on non-invasive approaches, is a relevant unsolved clinical need. Peripheral blood mononuclear cells (PBMC) from MS subjects harbor dysregulations in their transcriptional profiles (Srinivasan et al., 2017a; Srinivasan et al., 2017b), so that they may serve for machine learning-based classification of patients with distinct forms of disease (Acquaviva et al., 2020). Here we moved to whole blood transcriptomics to select transcriptional signatures predicting CIS conversion and MS state.

2. Materials and mehods

2.1. Human subjects

The study included initially 225 individuals, comprising subjects with CIS, RR-MS patients and healthy controls (HC). This research was conducted according to the principles expressed in the Declaration of Helsinki and after approval of the Ethics Committees of involved hospitals. Written informed consent was obtained from all participants. Sex at birth and age were collected from all subjects, while information on gender and socioeconomic status was not under analysis. All healthy individuals had no acute or chronic inflammatory or autoimmune disorders at the time of blood sampling. CIS subjects had a recent first neurological episode with symptoms suggestive of demyelination, they were with or without white matter (WM) brain MRI abnormalities and those without brain MRI lesions had spinal cord lesions. Oligoclonal bands in the liquor and serum were checked by standard diagnostics, and 68 CIS and 53 RR-MS patients resulted positive. Blood sampling for deep RNA sequencing was performed between month 1 and 3 from the first clinical event in most cases. All CIS and RR-MS subjects were clinically stable at the time of blood sampling (defined as no relapses and no steroid treatment in the month before sampling), were not suffering from any other acute or chronic inflammatory/autoimmune diseases and were not under any disease-modifying treatment (treatment naïve in most cases except for 4 RR-MS patients). RR-MS subjects were distinct from the CIS cohort and had median disease duration of 2.01 $\pm$ 4.86 years. Median time between the last relapse and blood sampling was 6.39 $\pm$ 32.20 months. Peripheral blood was collected into PAXgene Blood RNA Tubes (Qiagen) between 9 and 12 a.m. Clinical follow up of CIS subjects was performed every three months for the first year and then yearly unless neurological deterioration emerged. Brain and spinal cord MRI scans were acquired using 1.5 or 3.0 Tesla scanners using standardized protocols. More specifically, for the brain, axial dual-echo (DE) and/or fast fluid-attenuated inversion recovery (FLAIR) and post-contrast (0.1 mmol/kg of gadolinium [Gd]-DTPA; acquisition delay: $\approx$ 10 min) T1-weighted sequences were acquired at baseline and at follow-up. Slice thickness varied between 3 and 5 mm, in-plane resolution between 0.45 and 1.0 mm, no gap between slices. For the spinal cord, sagittal short tau inversion recovery (STIR) and/or T2-weighted and post-contrast T1-weighted sequences (0.1 mmol/kg of gadolinium [Gd]-DTPA; acquisition delay: 5 min) with 3 mm slice thickness, in-plane resolution between 0.4375 and 1.0 mm, no gap between slices, covering the cervical and thoracic cord were acquired. All images were assessed by consensus by two experienced observers, blinded to the patients' identity and MS status at the Neuroimaging Research Unit (Milan, Italy). Brain white matter (WM) lesions were identified on dual-echo/FLAIR images and were defined as hyperintensities involving at least 3 voxels, present on at least two slices and visible on two different sequences (e.g., FLAIR and T2 or proton density and T2). Spinal cord lesions were identified on sagittal short tau inversion recovery (STIR) and/or T2-weighted sequences. Total number of WM lesions, number of periventricular (abutting the lateral ventricles without intervening WM), juxtacortical (touching the cortex), cortical (within the cortex), posterior fossa (located in the brainstem, cerebellar peduncles and cerebellar hemispheres) and spinal cord lesions were evaluated following published recommendations (Filippi et al., 2019). Gd-enhancing lesions (area of hyperintensity on post-contrast T1-weighted images) were identified on post-contrast T1-weighted scans. On the MRI scan acquired at follow-up, the numbers of new T2-hyperintense and Gd-enhancing lesions were quantified.

2.2. Generation of whole blood RNA for sequencing experiments

RNA extraction was conducted using PAXgene Blood RNA Kit (Qiagen). RNA quantification was performed on Nanodrop (Thermo Fisher Scientific) and quality control was conducted using Bioanalyzer 2100 with Agilent RNA 6000 Nano Kit (Agilent). RNA integrity (RIN) values were all above 8. RNA samples were processed with Globin-Zero™ Gold Kit (Illumina) to remove rRNA and globin mRNA.

2.3. RNA seq experiment, quality controls and data processing

Sequencing libraries were generated using TruSeq Stranded mRNA Library Prep (Illumina) following manufacturer's instructions. Paired-end RNA sequencing was performed with NovaSeq 6000 technology (Illumina) and reached an average depth of 45 million reads. Initial RNAseq quality control (QC) checks included evaluation of GC and per-base sequence content using FastQC (v0.11.9). All raw reads that passed initial QC were aligned to the human reference genome (hg38/GRCh38) using STAR (v2.5.3a). Post-alignment QC including quantification of mapped reads on unique regions and coding sequences was conducted using the MultiQC (v1.9.0) tool. Gene expression quantifications (raw read counts) were calculated using the function featureCounts from R package Rsubread (v1.22.2) and Gencode v28 basic annotation, and pseudogenes were removed. Transcriptome datasets reached at least 10 million reads for 90 % of included samples.

2.4. Generation and processing of training and validation datasets for classifier development

For the generation of the final transcriptome dataset, transcripts were retained if expressed in at least 55 subjects (the number of subjects in the smallest group in the data, HC) according to R package edgeR (v3.26.8). Next, CPM (Count-per-million) were calculated for the retained transcripts. For outlier detection the distance among all subjects was calculated using Pearson correlation coefficient and Z scores were calculated for correlation matrix. Subjects with Z score less than -2 were identified as outliers (5 CIS and 2 RR-MS) and excluded from the analysis. The final dataset used for machine learning studies included 218 individuals, comprising 94 CIS subjects, 69 RR-MS patients and 55 healthy controls (HC) (Table S1). Raw read counts were then transformed into transcripts per kilobase million (TPM) to correct for both sequencing depth and gene length. Then, each class was divided in training and validation cohorts avoiding clinical, age and sex biases for proper model development. A TPM value $\geq$ 2 was applied to training sets and between-sample normalization was avoided to assure complete independence between training and validation data sets.

2.5. Machine learning pipeline

To construct binary classifiers, our previously developed machine

learning workflow (Acquaviva et al., 2020) was assembled using Python with implementations for AdaBoost-FT, AdaBoost-DC and RF algorithms. A ten-fold stratified NCV provided hyper-parameter optimization on different partitions of training data and a set of hyperparameters which maximised F-measure (harmonic mean of precision and recall) was selected as optimal hyperparameters. Hyper-parameters used for AdaBoost-FT were the number of iterations (I=2 to 10; step = 1) and the learning rate (h = 0.2 to 0.9; step = 0.1). Resampling instead of reweighting was applied to AdaBoost as it showed superior performance. Hyper-parameters used for RF were the number of trees (nt = 500 to 2000; step = 500) and the number of selected features (mtry = 50 to 300; step = 50; where sqrt of nTot features = 100). Hyper-parameters used for AdaBoost-DT were the number of iterations (I=2 to 10; step = 1) and the learning rate (h = 0.2 to 0.9; step = 0.1). The model with the best hyperparameters was re-trained on the whole training set and applied to the independent test set for final validation. To build more robust classifiers we repeated this procedure with a set of features that contributed more than 2 times to the classifier nodes. Precision-recall curves and AUPRC were generated using Python package matplotlib. Alternatively, numpy and scikit-learn packages were introduced in Python and applied to generate random combinations of 107 transcripts (1000 iterations) from the whole transcriptome devoid of the predictive RR-MS features before running the binary classification pipeline. Then, models were built on the training set by AdaBoost algorithm with the same hyperparameters optimized for the predictive RR-MS signature and validated on the independent test set. Sklearn.metrics package in Python was used to calculate and plot accuracy and confidence interval.

To build time-to-event classifiers, we developed a highly customized machine learning pipeline by adapting and extending the R code developed by Heider et al.(Haider et al., 2020) for the construction of "individual survival time distribution" (ISD) models. A schematic representation of the resulting pipeline is shown in Fig. 3A. We assembled a 10-fold stratified cross validation (CV) loop for hyperparameter optimization and comparison of three distinct machine learning algorithms: RSF, gbmCoxPH and CoxPH_KPEN. In the first step, data were split into training (63) and test (31) set and hyperparameter optimization was performed using the training dataset. Eventually, we used Gradient Boosting with Component-wise Linear Model (glmboost) using mboost package to achieve proper feature selection in ultra-high dimensional settings and adapted it to treat time-to-event censored data through the application of inverse probability of censoring weights. Feature selection was performed on the whole training set to avoid any information leakage and bias during optimization. Hyperparameters were number of trees (nt = 9000 to 18000; step = 3000), number of selected features (mtry = 20 to 30; step = 5) and node size (size = 5 to 15; step = 5). The optimization CV loop was designed to find the combination of hyperparameters that minimize the prediction error of each candidate model, calculated as 1- Concordance index (C-index). The C-index, a goodness of fit measure commonly used to evaluate risk models in survival analysis, was employed to evaluate model performance.

To examine the power of paraclinical features in predicting MS conversion, we designed a time-to-event experiment using positivity for oligoclonal bands in liquor and presence of MS lesions at distinct central nervous system locations at the first clinical event as features. Moreover, we tested whether these paraclinical measures could improve the prediction power of whole blood-derived transcripts by applying the time-to-event workflow to aggregated data.

pca3d package (v0.10.2) in R was used for PCA plots, while the ggplot2 package (v3.3.6) was applied for other plots. Differential expression analysis was performed for selected features by unpaired *t*-test for normally distributed data or Mann-Whitney *U* test in case of non-normal distribution. Functional annotation was performed using ToppGene Suite (https://toppgene.cchmc.org/).

3. Results

3.1. Inspection of global blood transcriptomes showed separation of RR-MS from CIS and healthy controls

More than 200 subjects, including treatment-naïve relapsing-remitting (RR) MS patients, CIS patients and sex- and age-matched healthy controls (HC), were recruited for this study and whole blood was collected into Pax-gene Blood RNA tubes during remission for RR-MS subjects and between month 1 and 3 from the first clinical event for CIS subjects (see Methods for details). After removal of rRNA and globin mRNA, RNA specimens were processed for deep paired-end RNA sequencing with NovaSeq 6000 technology, which reached an average of 45 million reads per sample. After alignment to human reference genome hg38/GRCh38 and removal of non-expressed transcripts and outliers (see Methods for details), the resulting global blood transcriptomes were grouped according to class (Fig. 1A) and inspected by principal component analysis (PCA). The PCA plot displayed clear separation of RR-MS from HC and CIS subjects, while minor distances existed between CIS and HC (Fig. 1B).

3.2. Binary models correctly distinguished relapsing-remitting MS from the healthy condition but were inaccurate in the prediction of early CIS conversion

To explore whether whole blood transcriptomes could discriminate RR-MS subjects from the healthy population, we divided the dataset into distinct training and test sets with similar demographic features (Table S1) and applied our previously published machine learning pipeline for binary classification (Acquaviva et al., 2020). Initially, we performed algorithm benchmarking using RNA-seq data of the training set and comparing the performance of three distinct machine learning algorithms (Random Forest RF, AdaBoost Functional Tree FT and AdaBoost Decision Tree DT) by nested cross validation (NCV) (Fig. 2A). During NCV the algorithm was trained, optimized and tested on different partitions of the training set for unbiased evaluation of the resulting classifier (Fig. 2A). Precision-recall curves and relative areas under the precision-recall curve (AUPRC) indicated high classification performance for the three algorithms in this task (Fig. 2B). Algorithms were then re-trained on the complete training set using the optimized parameters and applied to the independent test set for final validation (Fig. 2C). They generated very accurate models differentiating RR-MS from healthy subjects, with AdaBoost FT showing the best performance (Fig. 2D). Training of this algorithm on 90 blood transcriptomes relative to 49 RR-MS and 41 HC subjects extracted a model based on 107 transcripts, which correctly classified 14/14 healthy subjects and 19/20 RR-MS patients of the independent test set, resulting in exceptional precision (100 %), recall (95 %) and overall accuracy (97 %) (Fig. 3A). The same signature displayed modest prediction power (65 % accuracy) when AdaBoost algorithm was applied without hyperparameter optimization (Figure S2). As further control experiment, we implemented a Bootstrap approach for iterated random selection of 107 transcripts from the transcriptome deprived of the predictive RR-MS features, applied AdaBoost algorithm with hyperparameters optimized for the predictive signature and verified prediction accuracy of 1000 distinct random combinations of 107 transcripts on the test set. This experiment measured a mean accuracy of 75 % (95 % confidence interval 61–88 %) for the random selection of 107 features (Figure S3), thus proving that prediction obtained with the RR-MS signature was not due to chance.

PCA plots built on RR-MS features separated subjects according to disease state and not sex (Fig. 3B and C). These data indicate that MS is associated with clear predictive transcriptional signals in blood cells that may equally classify female and male patients. Among predictive transcripts, some were regulatory RNAs such as long non-coding RNAs, or RNAs coding for proteins involved e.g. in RNA metabolism and immune signaling (Fig. 3D, Table S2). Among the 107 features, 74 were

A

Class	n (female: male)	Age (mean, years)
CIS	94 (58:36)	33.68± 9.25
RR-MS	69 (38:31)	36.04 ± 9.49
HC	55 (30:25)	35.87 ± 11.45

B

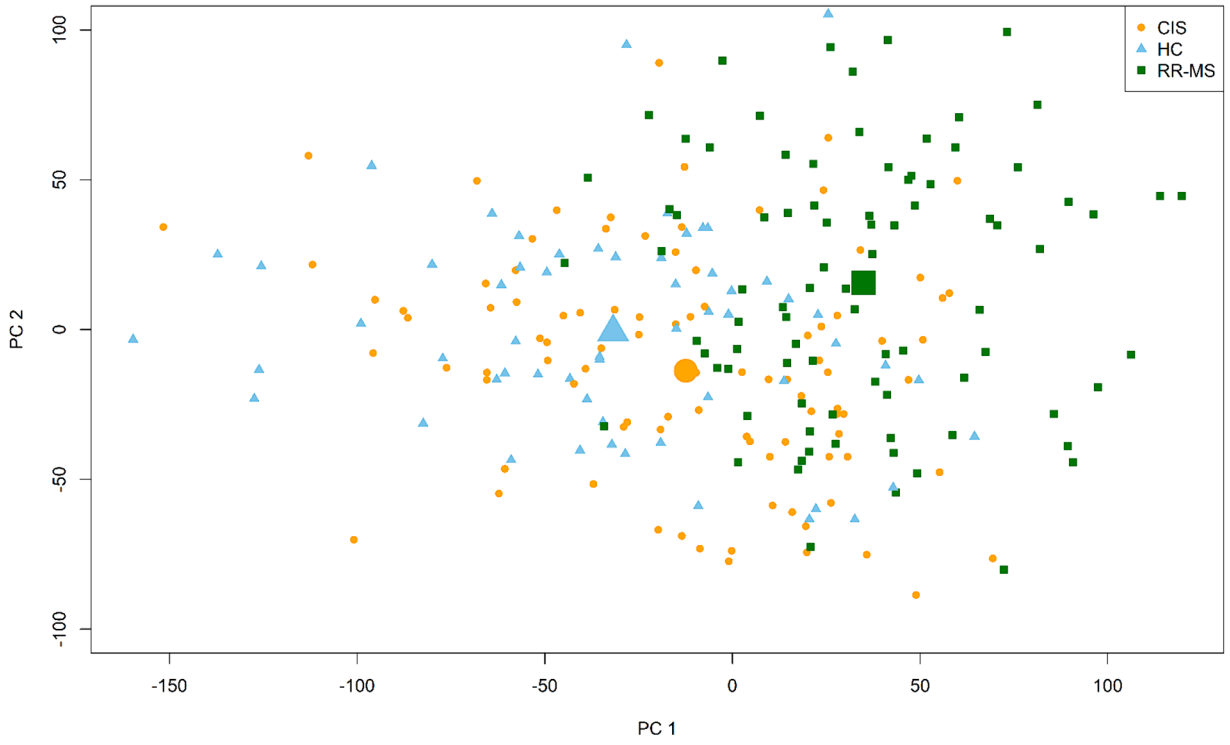

Fig. 1. Demographic features of the subjects included in the study and relative blood transcriptome distribution. A. Demographic characteristics of the subjects included in the study according to class. **B.** PCA plot of whole blood transcriptomes according to class (HC, blue; CIS, orange; RR-MS, green). Larger symbols indicate centroids.

differentially expressed between RR-MS and HC, with 48 upregulated and 26 downregulated transcripts in RR-MS (Table S2).

To assess whether the RR-MS model was already present at the onset of disease, we added 31 CIS blood transcriptomes to the test set and verified their classification by the RR-MS model. As shown in Fig. 3E, only 10 out of 31 CIS subjects were classified as RR-MS, indicating that this transcriptional model is suitable to identify definite RR-MS but is not reproduced in CIS yet.

As only a proportion of CIS subjects is going to develop MS, we investigated whether whole blood CIS transcriptome carried sufficient information to predict conversion from CIS to MS by 12 months from disease onset. Clinical and magnetic resonance imaging (MRI) follow-up examinations of CIS subjects were performed as described in methods, and conversion status was defined according to the 2010 revision of McDonald diagnostic criteria (Filippi et al., 2022). We then applied our binary classification pipeline to transcriptomes of early converters (named Conv CIS), who developed MS within 12 months from the first episode, and compared them to those of CIS subjects who developed MS after 12 months or were still not converted at the last follow up visit (named nonConv CIS, Fig. 3F). Algorithm training on 63 blood transcriptomes led to the definition of a 58 transcript-based signature, which however classified correctly only 2 out of 12 Conv CIS and 16 out of 19 nonConv CIS of the independent test set, resulting in low precision (40 %) and accuracy (58 %). Thus, early converters to MS are not identified when analyzing blood transcriptome with the conventional binary classification following an arbitrary conversion time threshold.

3.3. Time-to-event models predicted conversion to MS more reliably when based on blood transcriptomes than on paraclinical data at the first clinical episode

Conversion time to MS is a continuous variable, which may greatly vary among the patients as shown also for our cohort (Fig. 1S). Time-to-event analysis, which integrates occurrence of the event of interest with a range of time, includes statistical tools for machine learning approaches and has found some application in medicine (Wang et al., 2019). To overcome limitations of the binary classification paradigm in the prediction of CIS conversion to MS, we assembled a time-to-event machine learning framework (Fig. 4A, Table S3), which exploited temporal information relative to the conversion event for each CIS subject,

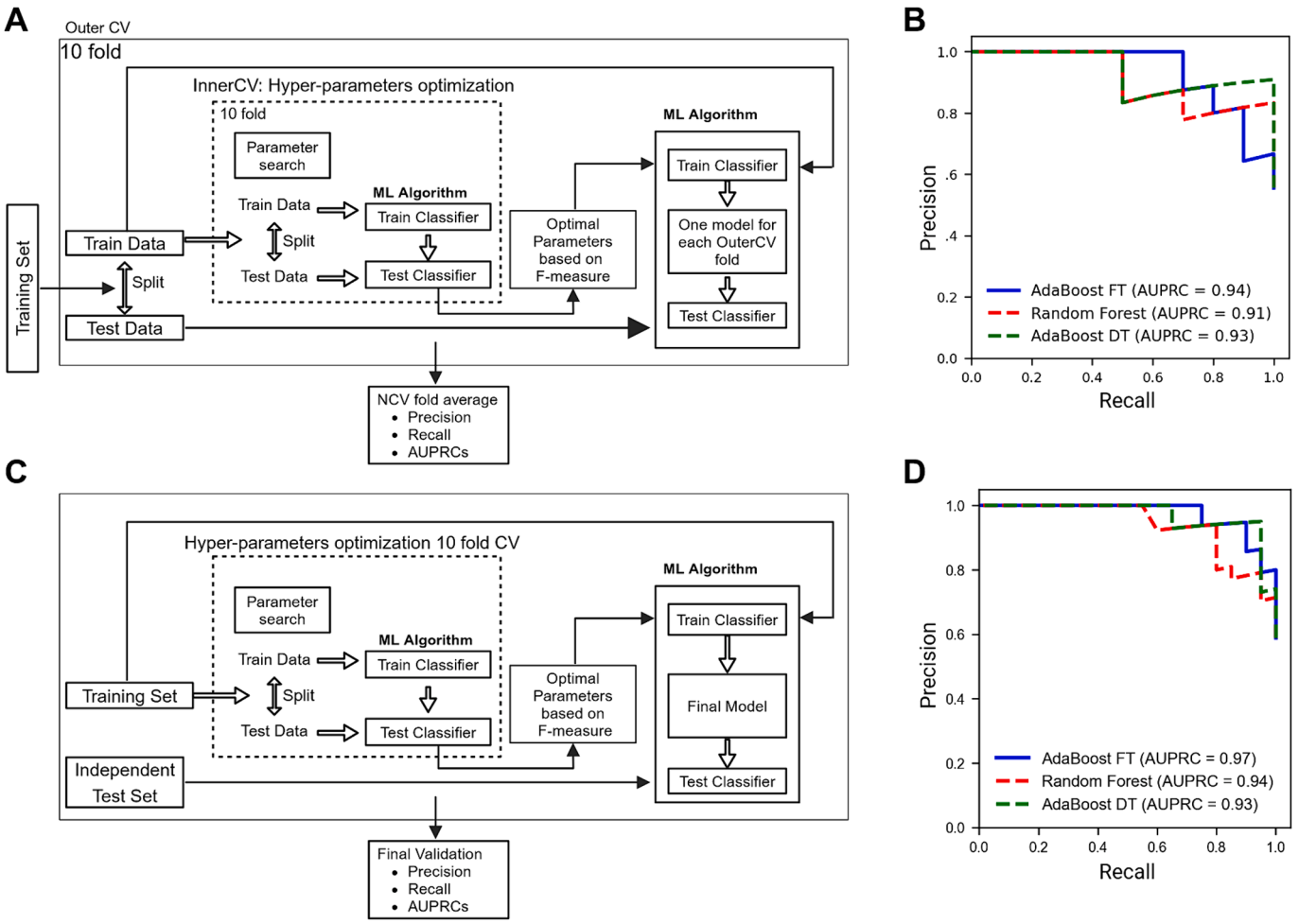

Fig. 2. Machine Learning Pipeline for binary classification. A. Nested cross-validation (NCV) for algorithm benchmarking. At each fold of the outer CV, transcriptomic data of the training set are split in two sub-sampled datasets, one for training and the other for testing. The sub-sampled training set enters the hyper-parameter optimization loop for three machine learning algorithms (AdaBoost-FT, AdaBoost-DT, and RF algorithms), where it is further split into training and test partitions following a second 10-fold CV (inner CV), where different combinations of hyper-parameters are evaluated (one 10-fold CV for each combination). The combination of hyper-parameters that maximize the F-measure (harmonic mean of precision and recall) of the class of interest is retained as optimal, applied to the algorithm, and tested on the test set of the corresponding outer CV fold. The entire procedure is repeated 10 times, and the averaged performance is collected at the end of the outer CV loop and used for algorithm comparison. **B.** Comparison of the performance obtained by the three algorithms in the NCV experiment on the training set is shown as precision-recall (PR) curves and relative areas under the curves (AUPRCs). **C.** Final optimization and validation of the models. The whole training dataset enters the hyper-parameter optimization loop, where it is subjected to the search for the combination of hyper-parameters that maximize the F-measure. The optimal hyper-parameters are applied to the algorithm, which is trained on the whole training set and tested on the independent test set for final validation. **D.** Comparison of the performance of the different algorithms on the independent test set for RR MS versus HC classifiers.

thus producing time-dependent and subject-specific survival probability curves. Three distinct time-to-event algorithms (Random Survival Forests RSF, Gradient Boosting Machines combined with Cox Proportional Hazards gbmCoxPH and CoxPH_KPEN) were initially trained, optimized and tested on blood transcriptomes derived from different partitions of the training set in a 10-fold CV loop (Fig. 4A, Table S3). The models were then re-trained on the complete training set using the optimized parameters and applied to the independent test set for final validation (Fig. 4A). As shown in Table S4, the three algorithms reached scarce C-index values both in the CV experiment with the train set and on the test set. Introduction of a feature selection step by glmboost algorithm before time-to-event algorithm benchmarking improved performance of CoxPH_KPEN on the training set (C-index = 87.3 %) which was however not confirmed with the test set (C-index = 54.2 %), demonstrating model overfitting to the training set. Importantly, the RSF algorithm led to personalized transcripts-based survival curves (Fig. 4C) reaching a C-index of 74.3 % in the independent test cohort when trained with the 58 glmboost-selected transcriptional features (Fig. 4B). The same pipeline constructed a model with scarse performance on the independent test when conversion time and event were defined according to more recent diagnostic criteria (C-index = 56.4 %, Table S5). Most of the 58 predictive features (60.34 %) belonged to regulatory RNAs such as microRNAs and long non-coding RNAs (Fig. 4D, Table S6). Functional annotation confirmed that the conversion signature was significantly enriched in members of the microRNA gene family (FDR-corrected p-value 9.740e-7).

We then examined the contribution of paraclinical data (positivity for oligoclonal bands in liquor and presence of periventricular, juxtacortical, infratentorial brain lesions and/or spinal cord lesions as detected by MRI) measured at the first clinical episode to the prediction of CIS conversion. Time-to-event analysis using the RSF algorithm on paraclinical features constructed a model with moderate performance on the independent test cohort (C-index = 70.5 %, Fig. 4B). Addition of demographic and/or paraclinical features to the previously selected 58 transcript-based signature reached a C-index of about 72 % (Fig. 4B), indicating that blood transcriptional features are sufficient to obtain conversion risk prediction and that this model is not influenced by sex and age of the subjects.

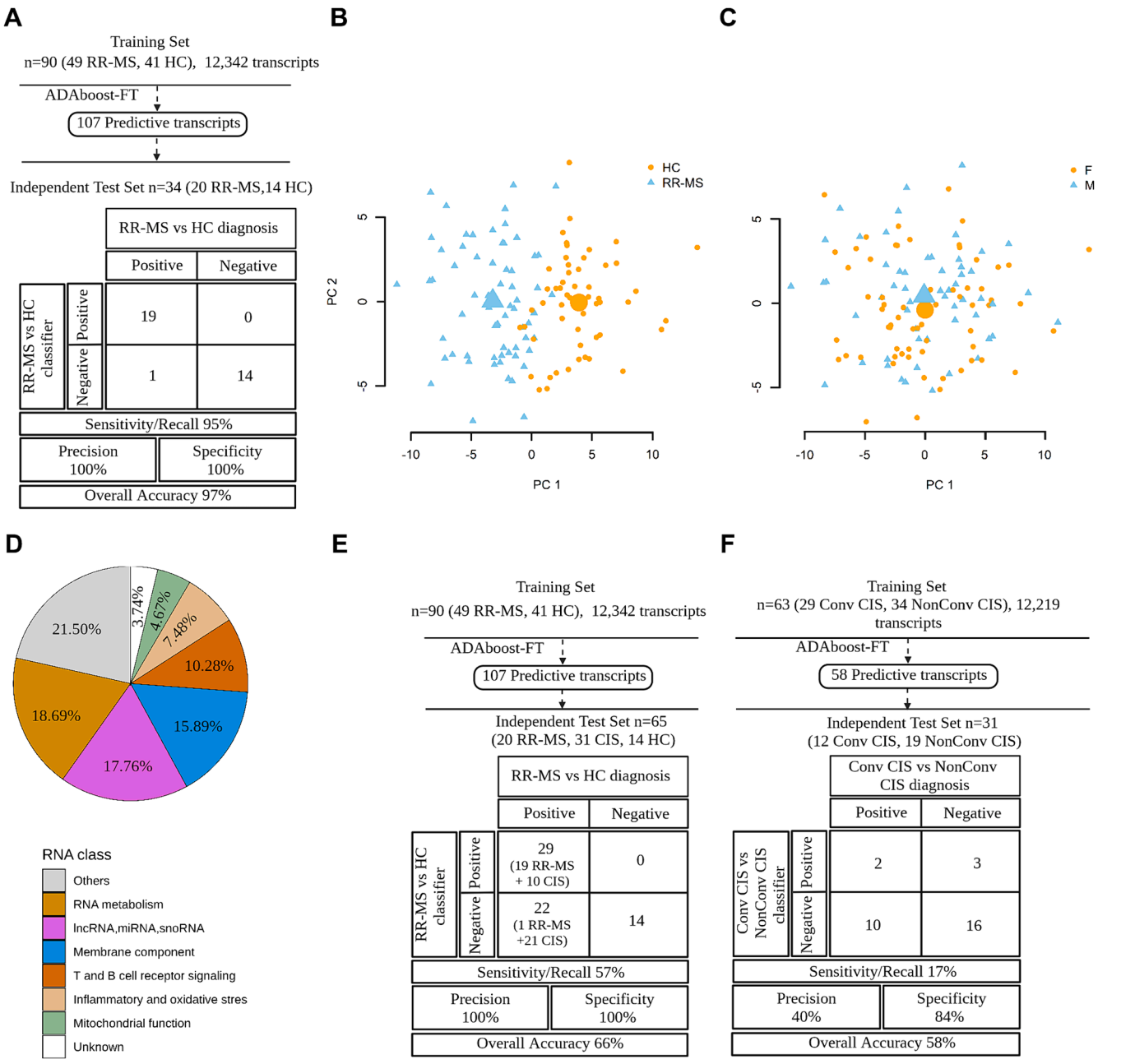

Fig. 3. Machine learning-based binary classification of CIS and RR-MS state from blood transcriptome. A. Identification of binary classifiers from whole blood transcriptomes discerning RR-MS subjects from the healthy population. **B-C.** PCA plots generated by the predictive 107 transcriptional features when classifying disease state (B) or sex (C). Larger symbols indicate centroids. **D.** Main RNA classes within 107 transcript-based RR-MS signature. **E.** Application of RR-MS vs. HC model to an independent test set including 31 CIS blood transcriptomes. **F.** Binary classification to predict early converters (Conv CIS) and non converters (non-Conv CIS).

4. Discussion

Here we found that whole blood transcriptomes deliver key predictive information about multiple sclerosis risk and state that can be reproducibly captured and validated by artificial intelligence.

Given the importance of MRI in MS diagnosis, prognosis and treatment monitoring, the majority of published prediction tasks by machine learning focused on MRI data, alone or jointly with clinical data (Bonacchi et al., 2022). Regarding MS diagnosis, no validated models were developed to distinguish MS from healthy subjects despite the good prediction accuracy shown by cross-validation studies using conventional (Bonacchi et al., 2022; Eitel et al., 2019; Lopatina et al., 2020) or advanced (Yoo et al., 2018; Zurita et al., 2018) MRI data, as their applicability suffers from the difficulty to obtain reproducible and repeated MRI measurements and cover relative costs. Promising classification results were also obtained when analyzing paraclinical cerebrospinal fluid and/or blood parameters (Barbour et al., 2017; Goyal et al., 2019; Gross et al., 2021). Our group recently demonstrated that PBMC carry transcriptional markers shared among MS stages and forms that can predict MS diagnosis with 89 % accuracy in an independent test set including healthy people and subjects with MS or other neurological disorders (Acquaviva et al., 2020). Here, to reduce blood sample processing and exploit deep RNA sequencing, we generated large and accurate whole blood mRNA repertoires from RR-MS and healthy subjects suitable for our machine learning binary classification pipeline. The model displayed 97 % accuracy on the independent test set,

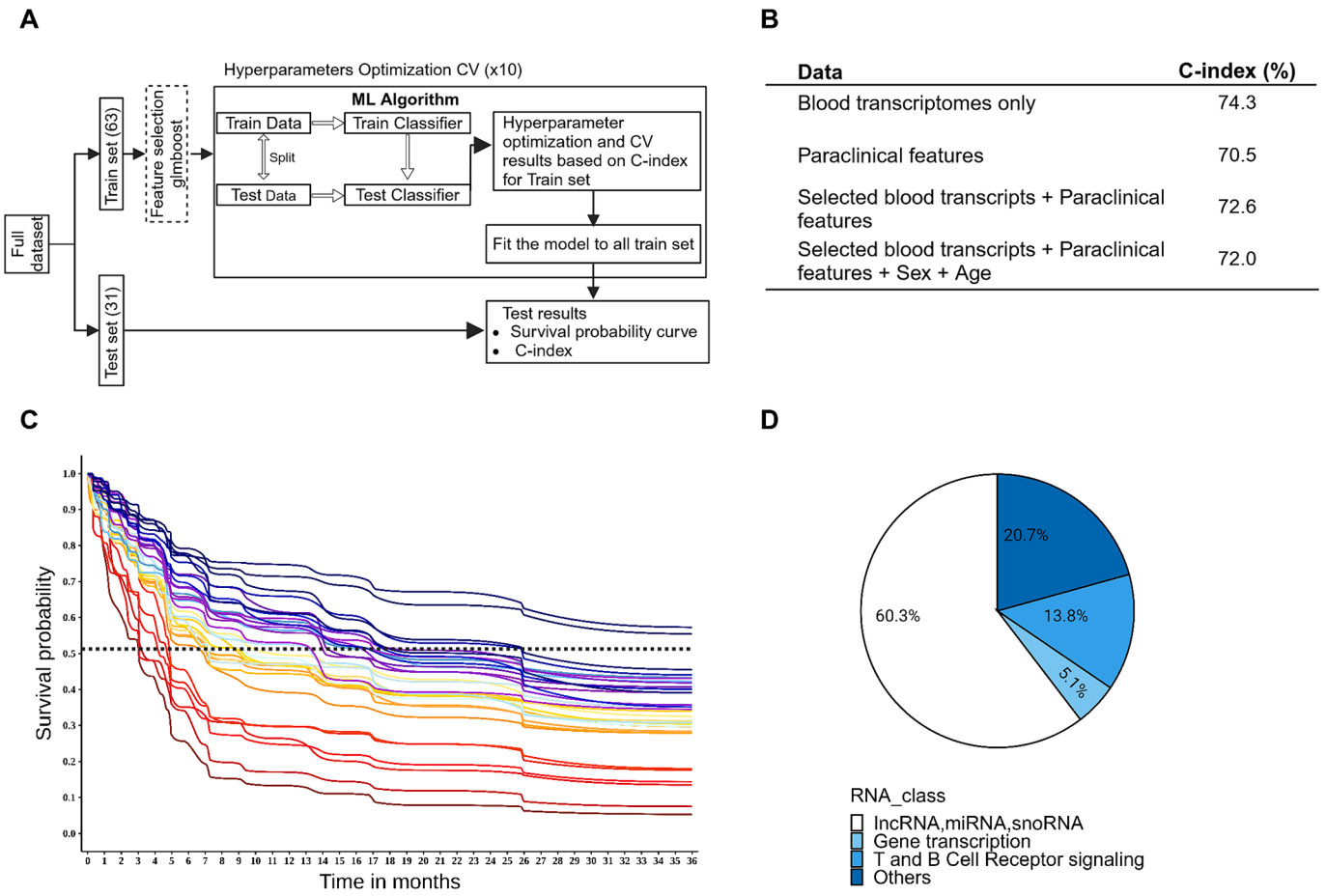

Fig. 4. Machine learning-based Time-To-Event analysis of CIS conversion. A. Workflow for machine learning-based Time-To-Event analysis of CIS data. The initial transcriptomics dataset is partitioned into distinct training and test sets with similar demographic and clinical features (Table S3). For algorithm optimization and comparison the training set enters a hyper-parameter optimization loop, where it is further divided into training and test partitions through 10-fold cross-validation. The hyper-parameter combination minimizing prediction errors is then applied to the algorithms, which are trained on the whole training set and tested on the independent test set. Eventually, a feature selection step with glmboost algorithm is applied before algorithm benchmarking. **B.** Performance of RSF-based model when applied to CIS data (blood transcriptomes and/or paraclinical data eventually with demographic features) obtained at the first episode. **C.** RSF-based survival probabilities for 31 CIS subjects of the independent test set. **D.** Main RNA classes within the 58 transcript-based CIS signature.

demonstrating that the analysis of whole blood instead of PBMC or specific immune cell subsets did not result in the loss of predictive information and that a single blood sample was sufficient to assess disease state. A good proportion of predictive markers were lncRNA, miRNA, snoRNA, others coded for proteins involved in processes known to be altered in MS, including inflammatory and oxidative stress (i.e. MS-associated upregulation of CARD16 (Karasawa et al., 2015; Musella et al., 2020) and RORC (Capone & Volpe, 2020), and down-regulation of PRXL2A/FAM213A (Guo et al., 2015) and NQO1 (Dinkova-Kostova & Talalay, 2010;van Horssen et al., 2011)), mitochondrial function (i.e. APOO (Tang et al., 2023) and COX8A (Hallmann et al., 2016; Gonzalo et al., 2019) both upregulated in RR-MS transcriptomes), innate immunity and antigen presentation (downregulation of CCL28 (Mohan et al., 2017) and upregulation of CLN3 (Hersrud et al., 2016)), CD8 T cell exhaustion (i.e. upregulation of HMGB2 (Neubert et al., 2023; Smolders & Hamann, 2022)) and IgA synthesis (upregulation of IGHA1 (Boussamet et al., 2022)).

Machine learning-based imaging diagnostics in patients with a clinically isolated syndrome showed modest (65–70 %) accuracy in predicting clinical conversion to MS in cross-validation binary classification experiments using baseline MRI data (Bendfeldt et al., 2019; Wottschel et al., 2019). Though accurate in discriminating RR-MS from the healthy population, our MS blood RNA signature was ineffective to predict CIS converters from non converters. Conversion time, however, follows a continuous, not binary distribution, urging the development of novel machine learning pipelines incorporating conversion time into analysis. Here we described a time-to-event machine learning workflow which leveraged conversion status together with conversion time and analyzed different types of data, including demographic, paraclinical and blood transcriptome parameters. Comparison of distinct diagnostic criteria indicated the existence of biological correlates in blood transcriptomes for 2010 and not 2017 clinical criteria. This is not unexpected as 2017 criteria were developed to maximize therapeutic care and therefore suffer from low specificity (Filippi et al., 2022). Interestingly, the best classification result in the independent test set was obtained by the signature based on transcriptional markers only. Most of them were regulatory RNAs, while others coded for proteins involved in e.g. antigen presentation (HLA-DQB2 (Ferrè et al., 2020)), complement activation (C4BPA (Werner & Criss, 2023)), γ/δ T cell function (TRGV4 (Reijneveld et al., 2020), TRGV5 (McKenzie et al., 2022) and BTNL3 (Willcox et al., 2019)), immunoregulation (TMEM176B, (Hill et al., 2022) and PTGES (Loynes et al., 2018)), antiviral responses (ARHGDIA, (Cohn et al., 2022), ATOH8 (Liu et al., 2023), BEX1 (Martens et al., 2022)), processes which still need investigation in early MS.

In conclusion, here we describe that blood transcriptomics analyzed by artificial intelligence identifies predictive markers providing 97 % accuracy for definite MS. This information extends to whole blood the observation about relevant changes in peripheral immunity previously

described for PBMC transcriptomes (Acquaviva et al., 2020). The MS transcriptional signature is however ineffective for the CIS stage, suggesting that time and disease evolution are necessary to fix it in blood cells. We also provide the first proof-of principle study where application of machine learning-based time-to-event analysis to whole blood transcriptomes can predict personalized conversion risks with good accuracy. Clearly, despite the current project already analyzed deep RNA sequencing and paraclinical data relative to more than 90 CIS subjects, future studies with larger cohorts are necessary to further optimize and validate the model. However, compared to the current diagnostic path, which requires several clinical follow-up examinations, the advantage of our approach is that blood transcriptome-based models can be captured at the first clinical event and predict more efficiently than paraclinical features at baseline, thus allowing early definition of risk of conversion to MS. Prospectively the described machine learning pipelines may be applied to verify whether blood transcriptomics may support the specific identification of MS from other CNS demyelinating diseases such as neuromyelitis optica or myelin oligodendrocyte glycoprotein antibody-associated disease, or allow early prognostic stratification of MS according to disease activity and course.

CRediT authorship contribution statement

Maryam Omrani: Writing – original draft, Methodology, Formal analysis. **Rosaria Rita Chiarelli:** Writing – review & editing, Writing – original draft, Software, Methodology, Formal analysis. **Massimo Acquaviva:** Writing – original draft, Software, Resources, Methodology, Formal analysis. **Claudia Bassani:** Resources, Methodology, Data curation. **Gloria Dalla Costa:** Resources, Data curation. **Federico Montini:** Data curation. **Paolo Preziosa:** Data curation. **Lucia Pagani:** Software. **Francesca Grassivaro:** Investigation, Data curation. **Simone Guerrieri:** Data curation. **Marzia Romeo:** Investigation. **Francesca Sangalli:** Investigation, Data curation. **Bruno Colombo:** Investigation. **Lucia Moiola:** Software. **Mauro Zaffaroni:** Investigation. **Anna Pietroboni:** Investigation. **Alessandra Protti:** Investigation. **Marco Puthenparampil:** Resources. **Roberto Bergamaschi:** Investigation. **Giancarlo Comi:** Investigation, Funding acquisition. **Maria A. Rocca:** . **Vittorio Martinelli:** Resources, Methodology, Investigation, Data curation. **Massimo Filippi:** Writing – original draft, Software, Resources, Methodology, Formal analysis. **Cinthia Farina:** Writing – review & editing, Writing – original draft, Supervision, Resources, Methodology, Investigation, Funding acquisition, Conceptualization.

Declaration of competing interest

The authors declare that they have no known competing financial interests or personal relationships that could have appeared to influence the work reported in this paper.

Data availability

Data will be made available on request.

Acknowledgments

we acknowledge the Center for Omics Sciences at the IRCCS Ospedale San Raffaele (COSR), all the participants who donated blood for this study and Centro Sclerosi Multipla Ospedale San Raffaele.

Funding

Italian Ministry for Health (RF-2011-02349698, RF-2018-12367731).

Appendix A. Supplementary data

Supplementary data to this article can be found online at https://doi.org/10.1016/j.bbi.2024.07.039.

References

Acquaviva, M., Menon, R., Di Dario, M., Dalla Costa, G., Romeo, M., Sangalli, F., Colombo, B., Moiola, L., Martinelli, V., Comi, G., Farina, C., 2020. Inferring Multiple Sclerosis Stages from the Blood Transcriptome via Machine Learning. Cell Reports Medicine 1 (4). https://doi.org/10.1016/j.xcrm.2020.100053.

Barbour, C., Kosa, P., Komori, M., Tanigawa, M., Masvekar, R., Wu, T., Johnson, K., Douvaras, P., Fossati, V., Herbst, R., Wang, Y., Tan, K., Greenwood, M., Bielekova, B., 2017. Molecular-based diagnosis of multiple sclerosis and its progressive stage. Ann. Neurol. 82 (5), 795–812. https://doi.org/10.1002/ana.25083.

Bebo, B., Cintina, I., LaRocca, N., Ritter, L., Talente, B., Hartung, D., Ngorsuraches, S., Wallin, M., Yang, G., 2022. The Economic Burden of Multiple Sclerosis in the United States. Neurology 98 (18), e1810–e1817. https://doi.org/10.1212/WNL.0000000000200150.

Bendfeldt, K., Taschler, B., Gaetano, L., Madoerin, P., Kuster, P., Mueller-Lenke, N., Amann, M., Vrenken, H., Wottschel, V., Barkhof, F., Borgwardt, S., Klöppel, S., Wicklein, E.-M., Kappos, L., Edan, G., Freedman, M.S., Montalbán, X., Hartung, H.-P., Pohl, C., Nichols, T.E., 2019. MRI-based prediction of conversion from clinically isolated syndrome to clinically definite multiple sclerosis using SVM and lesion geometry. Brain Imaging Behav. 13 (5), 1361–1374. https://doi.org/10.1007/s11682-018-9942-9.

Bonacchi, R., Filippi, M., Rocca, M.A., 2022. Role of artificial intelligence in MS clinical practice. NeuroImage: Clinical 35. https://doi.org/10.1016/j.nicl.2022.103065.

Boussamet, L., Rajoka, M.S.R., Berthelot, L., 2022. Microbiota, IgA and Multiple Sclerosis. Microorganisms 10 (3). https://doi.org/10.3390/microorganisms10030617.

Capone, A., & Volpe, E. (2020). Transcriptional Regulators of T Helper 17 Cell Differentiation in Health and Autoimmune Diseases. In *Frontiers in Immunology* (Vol. 11). Frontiers Media S.A. https://doi.org/10.3389/fimmu.2020.00348.

Chung, K.K., Altmann, D., Barkhof, F., Miszkiel, K., Brex, P.A., O'Riordan, J., Ebner, M., Prados, F., Cardoso, M.J., Vercauteren, T., Ourselin, S., Thompson, A., Ciccarelli, O., Chard, D.T., 2020. A 30-Year Clinical and Magnetic Resonance Imaging Observational Study of Multiple Sclerosis and Clinically Isolated Syndromes. Ann. Neurol. 87 (1), 63–74. https://doi.org/10.1002/ana.25637.

Cohn, O., Yankovitz, G., Peshes-Yaloz, N., Steuerman, Y., Frishberg, A., Brandes, R., Mandelboim, M., Hamilton, J.R., Hagai, T., Amit, I., Netea, M.G., Hacohen, N., Iraqi, F.A., Bacharach, E., Gat-Viks, I., 2022. Distinct gene programs underpinning disease tolerance and resistance in influenza virus infection. Cell Syst. 13 (12), 1002–1015.e9. https://doi.org/10.1016/j.cels.2022.11.004.

Dinkova-Kostova, A. T., & Talalay, P. (2010). NAD(P)H:quinone acceptor oxidoreductase 1 (NQO1), a multifunctional antioxidant enzyme and exceptionally versatile cytoprotector. In *Archives of Biochemistry and Biophysics* (Vol. 501, Issue 1, pp. 116–123). https://doi.org/10.1016/j.abb.2010.03.019.

Eitel, F., Soehler, E., Bellmann-Strobl, J., Brandt, A.U., Ruprecht, K., Giess, R.M., Kuchling, J., Asseyer, S., Weygandt, M., Haynes, J.D., Scheel, M., Paul, F., Ritter, K., 2019. Uncovering convolutional neural network decisions for diagnosing multiple sclerosis on conventional MRI using layer-wise relevance propagation. Clinical, NeuroImage, p. 24.

Ferrè, L., Filippi, M., Esposito, F., 2020. Involvement of Genetic Factors in Multiple Sclerosis. Front. Cell. Neurosci. 14 https://doi.org/10.3389/fncel.2020.612953.

Filippi, M., Preziosa, P., Banwell, B.L., Barkhof, F., Ciccarelli, O., De Stefano, N., Geurts, J.J.G., Paul, F., Reich, D.S., Toosy, A.T., Traboulsee, A., Wattjes, M.P., Yousry, T.A., Gass, A., Lubetzki, C., Weinshenker, B.G., Rocca, M.A., 2019. Assessment of lesions on magnetic resonance imaging in multiple sclerosis: practical guidelines. In: Brain, Vol. 142(7. Oxford University Press, pp. 1858–1875. https://doi.org/10.1093/brain/awz144.

Filippi, M., Preziosa, P., Meani, A., Costa, G.D., Mesaros, S., Drulovic, J., Ivanovic, J., Rovira, A., Tintorè, M., Montalban, X., Ciccarelli, O., Brownlee, W., Miszkiel, K., Enzinger, C., Khalil, M., Barkhof, F., Strijbis, E.M.M., Frederiksen, J.L., Cramer, S.P., Yousry, T., 2022. Performance of the 2017 and 2010 Revised McDonald Criteria in Predicting MS Diagnosis After a Clinically Isolated Syndrome. Neurology 98 (1), e1–e14. https://doi.org/10.1212/WNL.0000000000013016.

Gonzalo, H., Nogueras, L., Gil-Sánchez, A., Hervás, J.V., Valcheva, P., González-Mingot, C., Martin-Gari, M., Canudes, M., Peralta, S., Solana, M.J., Pamplona, R., Portero-Otin, M., Boada, J., Serrano, J.C.E., Brieva, L., 2019. Impairment of Mitochondrial Redox Status in Peripheral Lymphocytes of Multiple Sclerosis Patients. Front. Neurosci. 13 https://doi.org/10.3389/fnins.2019.00938.

Goyal, M., Khanna, D., Rana, P.S., Khaibullin, T., Martynova, E., Rizvanov, A.A., Khaiboullina, S.F., Baranwal, M., 2019. Computational intelligence technique for prediction of multiple sclerosis based on serum cytokines. Front. Neurol. 10 (JUL) https://doi.org/10.3389/fneur.2019.00781.

Gross, C.C., Schulte-Mecklenbeck, A., Madireddy, L., Pawlitzki, M., Strippel, C., Räuber, S., Krämer, J., Rolfes, L., Ruck, T., Beuker, C., Schmidt-Pogoda, A., Lohmann, L., Schneider-Hohendorf, T., Hahn, T., Schwab, N., Minnerup, J., Melzer, N., Klotz, L., Meuth, S.G., Wiendl, H., 2021. Classification of neurological diseases using multi-dimensional CSF analysis. Brain 144 (9), 2625–2634. https://doi.org/10.1093/brain/awab147.

Guo, F., He, H., Fu, Z.C., Huang, S., Chen, T., Papasian, C.J., Morse, L.R., Xu, Y., Battaglino, R.A., Yang, X.F., Jiang, Z., Xin, H.B., Fu, M., 2015. Adipocyte-derived PAMM suppresses macrophage inflammation by inhibiting MAPK signalling. Biochem. J 472 (3), 309–318. https://doi.org/10.1042/BJ20150019.

Haider, H., Hoehn, B., Davis, S., Greiner, R., 2020. Effective Ways to Build and Evaluate Individual Survival Distributions. In. J. Mach. Learn. Res. 21.

Hallmann, K., Kudin, A.P., Zsurka, G., Kornblum, C., Reimann, J., Stüve, B., Waltz, S., Hattingen, E., Thiele, H., Nürnberg, P., Rüb, C., Voos, W., Kopatz, J., Neumann, H., Kunz, W.S., 2016. Loss of the smallest subunit of cytochrome c oxidase, COX8A, causes Leigh-like syndrome and epilepsy. Brain 139 (2), 338–345. https://doi.org/10.1093/brain/awv357.

Hersrud, S.L., Kovács, A.D., Pearce, D.A., 2016. Antigen presenting cell abnormalities in the Cln3-/- mouse model of juvenile neuronal ceroid lipofuscinosis. Biochim. Biophys. Acta Mol. basis Dis. 1862 (7), 1324–1336. https://doi.org/10.1016/j.bbadis.2016.04.011.

Musella, A., Fresegna, D., Rizzo, F.R., Gentile, A., De Vito, F., Caioli, S., Guadalupi, L., Bruno, A., Dolcetti, E., Buttari, F., Bullitta, S., Vanni, V., Centonze, D., Mandolesi, G., 2020 Jan. 'Prototypical' proinflammatory cytokine (IL-1) in multiple sclerosis: role in pathogenesis and therapeutic targeting. Expert Opin Ther Targets 24 (1), 37–46. https://doi.org/10.1080/14728222.2020.1709823. Epub 2020 Jan 3 PMID: 31899994.

Hill, M., Russo, S., Olivera, D., Malcuori, M., Galliussi, G., & Segovia, M. (2022). The intracellular cation channel TMEM176B as a dual immunoregulator. In *Frontiers in Cell and Developmental Biology* (Vol. 10). Frontiers Media S.A. https://doi.org/10.3389/fcell.2022.1038429.

Karasawa, T., Kawashima, A., Usui, F., Kimura, H., Shirasuna, K., Inoue, Y., Komada, T., Kobayashi, M., Mizushina, Y., Sagara, J., Takahashi, M., 2015. Oligomerized CARD16 promotes caspase-1 assembly and IL-1β processing. FEBS Open Bio 5, 348–356. https://doi.org/10.1016/j.fob.2015.04.011.

Liu, X., Fan, Z., Chen, L., Yang, J., Cheng, J., 2023. ATOH8 promotes HBV immune tolerance by inhibiting the pyroptotic pathway in hepatocytes. Mol. Med. Rep. 28 (1) https://doi.org/10.3892/mmr.2023.13018.

Lopatina, A., Ropele, S., Sibgatulin, R., Reichenbach, J.R., Güllmar, D., 2020. Investigation of Deep-Learning-Driven Identification of Multiple Sclerosis Patients Based on Susceptibility-Weighted Images Using Relevance Analysis. Front. Neurosci. 14 https://doi.org/10.3389/fnins.2020.609468.

Loynes, C. A., Lee, J. A., Robertson, A. L., Steel, M. J., Ellett, F., Feng, Y., Levy, B. D., Whyte, M. K. B., & Renshaw, S. A. (2018). PGE 2 production at sites of tissue injury promotes an anti-inflammatory neutrophil phenotype and determines the outcome of inflammation resolution in vivo. In *Sci. Adv* (Vol. 4).

Marrie, R.A., Allegretta, M., Barcellos, L.F., Bebo, B., Calabresi, P.A., Correale, J., Davis, B., De Jager, P.L., Gasperi, C., Greenbaum, C., Helme, A., Hemmer, B., Kanellis, P., Kostich, W., Landsman, D., Lebrun-Frenay, C., Makhani, N., Munger, K. L., Okuda, D.T., Tremlett, H., 2022. From the prodromal stage of multiple sclerosis to disease prevention. Nat. Rev. Neurol. 18 (9), 559–572. https://doi.org/10.1038/s41582-022-00686-x.

Martens, C.R., Dorn, L.E., Kenney, A.D., Bansal, S.S., Yount, J.S., Accornero, F., 2022. BEX1 is a critical determinant of viral myocarditis. PLoS Pathog. 18 (2) https://doi.org/10.1371/journal.ppat.1010342.

McKenzie, D.R., Hart, R., Bah, N., Ushakov, D.S., Muñoz-Ruiz, M., Feederle, R., Hayday, A.C., 2022. Normality sensing licenses local T cells for innate-like tissue surveillance. Nat. Immunol. 23 (3), 411–422. https://doi.org/10.1038/s41590-021-01124-8.

Mohan, T., Deng, L., & Wang, B. Z. (2017). CCL28 chemokine: An anchoring point bridging innate and adaptive immunity. In *International Immunopharmacology* (Vol. 51, pp. 165–170). Elsevier B.V. https://doi.org/10.1016/j.intimp.2017.08.012.

Neubert, E.N., DeRogatis, J.M., Lewis, S.A., Viramontes, K.M., Ortega, P., Henriquez, M. L., Buisson, R., Messaoudi, I., Tinoco, R., 2023. HMGB2 regulates the differentiation and stemness of exhausted CD8+ T cells during chronic viral infection and cancer. Nat. Commun. 14 (1) https://doi.org/10.1038/s41467-023-41352-0.

Ng, H.S., Zhu, F., Zhao, Y., Yao, S., Lu, X., Ekuma, O., Evans, C., Fisk, J.D., Marrie, R.A., Tremlett, H., 2024. Adverse Events Associated With Disease-Modifying Drugs for Multiple Sclerosis. Neurology 102 (3), e208006.

Reijneveld, J.F., Ocampo, T.A., Shahine, A., Gully, B.S., Vantourout, P., Hayday, A.C., Rossjohn, J., Moody, D.B., Van Rhijn, I., 2020. Human γδ T cells recognize CD1b by two distinct mechanisms. Proc. Natl. Acad. Sci. 117 (37), 22944–22952. https://doi.org/10.1073/pnas.2010545117.

Smolders, J., Hamann, J., 2022. Programmed Cell Death Protein 1–Positive CD8+ T Cells in Multiple Sclerosis. Neurology Neuroimmunology & Neuroinflammation 9 (4), e1173.

Srinivasan, S., Dario, M.D., Russo, A., Menon, R., Brini, E., Romeo, M., Sangalli, F., Costa, G.D., Rodegher, M., Radaelli, M., Moiola, L., Cantarella, D., Medico, E., Martino, G., Furlan, R., Martinelli, V., Comi, G., Farina, C., 2017a. Dysregulation of MS risk genes and pathways at distinct stages of disease. Neurology: Neuroimmunology and NeuroInflammation 4 (3). https://doi.org/10.1212/NXI.0000000000000337.

Srinivasan, S., Severa, M., Rizzo, F., Menon, R., Brini, E., Mechelli, R., Martinelli, V., Hertzog, P., Salvetti, M., Furlan, R., Martino, G., Comi, G., Coccia, E., Farina, C., 2017b. Transcriptional dysregulation of Interferome in experimental and human Multiple Sclerosis. Sci. Rep. 7 (1) https://doi.org/10.1038/s41598-017-09286-y.

Stankiewicz, J.M., Weiner, H.L., 2020. An argument for broad use of high efficacy treatments in early multiple sclerosis. Neurology Neuroimmunology & Neuroinflammation 7 (1), e636.

Tang, X., Huang, Z., Wang, F., Chen, J., Qin, D., Peng, D., Yu, B., 2023. Macrophage-specific deletion of MIC26 (APOO) mitigates advanced atherosclerosis by increasing efferocytosis. Atherosclerosis 386. https://doi.org/10.1016/j.atherosclerosis.2023.117374.

van Horssen, J., Witte, M.E., Schreibelt, G., de Vries, H.E., 2011. Radical changes in multiple sclerosis pathogenesis. Biochim. Biophys. Acta (BBA) - Mol. Basis Dis. 1812 (2), 141–150. https://doi.org/10.1016/j.bbadis.2010.06.011.

Wang, P., Li, Y., Reddy, C.K., 2019. Machine Learning for Survival Analysis: A Survey. ACM Comput. Surv. 51 (6) https://doi.org/10.1145/3214306.

Werner, L.M., Criss, A.K., 2023. Diverse Functions of C4b-Binding Protein in Health and Disease. J. Immunol. 211 (10), 1443–1449. https://doi.org/10.4049/jimmunol.2300333.

Willcox, C.R., Vantourout, P., Salim, M., Zlatareva, I., Melandri, D., Zanardo, L., George, R., Kjaer, S., Jeeves, M., Mohammed, F., Hayday, A.C., Willcox, B.E., 2019. Butyrophilin-like 3 Directly Binds a Human Vγ4+ T Cell Receptor Using a Modality Distinct from Clonally-Restricted Antigen. Immunity 51 (5), 813–825.e4. https://doi.org/10.1016/j.immuni.2019.09.006.

Wottschel, V., Chard, D.T., Enzinger, C., Filippi, M., Frederiksen, J.L., Gasperini, C., Giorgio, A., Rocca, M.A., Rovira, A., De Stefano, N., Tintoré, M., Alexander, D.C., Barkhof, F., Ciccarelli, O., 2019. SVM recursive feature elimination analyses of structural brain MRI predicts near-term relapses in patients with clinically isolated syndromes suggestive of multiple sclerosis. NeuroImage: Clinical 24. https://doi.org/10.1016/j.nicl.2019.102011.

Yoo, Y., Tang, L.Y.W., Brosch, T., Li, D.K.B., Kolind, S., Vavasour, I., Rauscher, A., MacKay, A.L., Traboulsee, A., Tam, R.C., 2018. Deep learning of joint myelin and T1w MRI features in normal-appearing brain tissue to distinguish between multiple sclerosis patients and healthy controls. NeuroImage: Clinical 17, 169–178. https://doi.org/10.1016/j.nicl.2017.10.015.

Zurita, M., Montalba, C., Labbé, T., Cruz, J.P., Dalboni da Rocha, J., Tejos, C., Ciampi, E., Cárcamo, C., Sitaram, R., Uribe, S., 2018. Characterization of relapsing-remitting multiple sclerosis patients using support vector machine classifications of functional and diffusion MRI data. NeuroImage: Clinical 20, 724–730. https://doi.org/10.1016/j.nicl.2018.09.002.